Electronic Supplementary Material (ESI) for Nanoscale Horizons.

Supporting information

Green Synthesis of Iron-Doped Graphene Quantum Dots: An Efficient Nanozyme for Glucose Sensing

Xinqi Li[1], Guanyou Lin[1], Lijun Zhou[2], Octavia Prosser[1], Mohammad H. Malakooti[1,2,3]*, Miqin Zhang[1,3]*

[1]Department of Materials Science and Engineering, University of Washington, Seattle, WA 98195, USA

[2]Department of Mechanical Engineering, University of Washington, Seattle, WA 98195, USA

[3]Institute for Nano-Engineered Systems, University of Washington, Seattle, WA 98195, USA

* Corresponding Authors: malakoot@uw.edu and mzhang@uw.edu

Synthesis of Fe_3O_4 Nanoparticles (Iron oxide nanoparticles coated with chitosan and poly(ethylene glycol) (PEG) copolymer modified with catechol, IOCCP):

Polymer (chitosan and poly(ethylene glycol) (PEG) copolymer modified with catechol, CCP) Synthesis[1]:

1.3 mmol of chitosan oligosaccharide (2300 MW) was dissolved in 40 mL of DI water. Then, 8 mL of methanol was added dropwise. The pH of the solution was adjusted to 6.5 by hydrochloric acid. Next, aldehyde-activated methoxy PEG (13 mmol) and 3,4-dihydroxybenzaldehyde (5.2 mmol, DHBA) dissolved in 16 mL of DI water, were added dropwise to the chitosan solution and the mixture was allowed to react for 1 h.

1.0 M sodium cyanoborohydride (185 μL, diluted to 12 mL in DI water) was added dropwise to the solution and reacted for an additional 18 h. The resulting catechol-functionalized chitosan-PEG (CCP) was precipitated with acetone, collected with a Buchner funnel, washed three times with acetone to remove unreacted PEG, dried by vacuum, redispersed in DI water, and further purified using tangential flow filtration (TFF, Millipore, Billerica, MA) with a 5 k MW cutoff cassette. Finally, the purified polymers were freeze-dried and stored at −20 °C.

Synthesis of Fe_3O_4 nanoparticles coated with CCP (IOCCP):

Iron oxide nanoparticles coated with CCP were synthesized through sonochemical coprecipitation of iron chlorides in aqueous solution. Briefly, 25 mg of pure CCP was mixed with iron chlorides (9 mg Fe(II), 18 mg Fe(III)) in 2.18 mL of degassed DI water. A 14.5 M solution of ammonium hydroxide was titrated slowly at 40 °C with sonication (40 kHz, 110 W) provided by a Branson ultrasonic bath (Danbury, CT) until a final pH of 10.5 was achieved to promote the nucleation of superparamagnetic iron oxide nanoparticles (SPIONs). The sonication was then continued until the pH reached 8.5−9.5 due to the evaporation of ammonia from the solution. For a typical synthesis, titration and sonication occurs concurrently for ∼30 min with sonication continuing for ∼10 min post-titration. The total sonication time is held constant at 40 min. Subsequently, 50 mg of additional CCP was added and the SPIONs were incubated overnight at 4 °C.

To purify the synthesized iron oxide nanoparticles coated with CCP (IOCCPs), the mixture was first subjected to centrifugation at 3500 rcf for 10 min, and the supernatant was further purified using size exclusion chromatography with S-200 resin (GE Healthcare, Piscataway, NJ) into 20 mM HEPES buffer, pH 7.4.

Catalase-like Activity of FeN/GQDs:

The catalase (CAT)-like activity was evaluated based on the fluorescent method. H_2O_2 can decompose into •OH, which interacts with terephthalic acid (TA), resulting in the formation of fluorescent 2-hydroxyterephthalic acid with an excitation wavelength at 320 nm and emits light at a peak of 425 nm. PBS buffer (100 mM, pH 7.4) containing H_2O_2 (10 mM) was vortexed with varying concentrations of

FeN/GQDs. Subsequently, TA solution (30 µL, 62.5 mM) was added at 25°C. The fluorescence of the resulting mixture was then measured after an incubation period of 6 hours.

Superoxide Dismutase-like Activity of FeN/GQDs:

The superoxide dismutase (SOD)-like activity was investigated via a fluorescent method. The reduction in O2- was assessed by quantifying the fluorescence intensity of ethidium, a product generated from the oxidation of Dihydroethidium (HE) by O2-. In a standard procedure, 0.6mM xanthine underwent a reaction in the presence of 0.05U/mL xanthine oxidase within a 100 mM pH 7.4 PBS buffer solution at 37°C for 30 minutes. A specific quantity of FeN/GQDs and 0.2 mg/mL HE was introduced. The solution was then transferred for fluorescence measurement after an incubation period of 40 minutes.

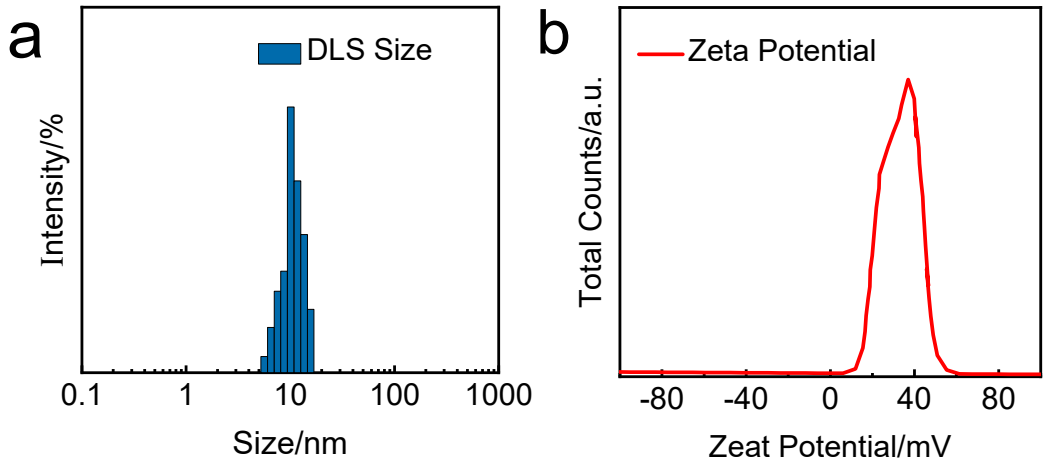

Figure S1. DLS data of FeN/GQDs. a) Hydrodynamic diameter shows an average size of 15.6 nm (b) Zeta potential shows a 39.4 mV which is a stable value for colloidal system.

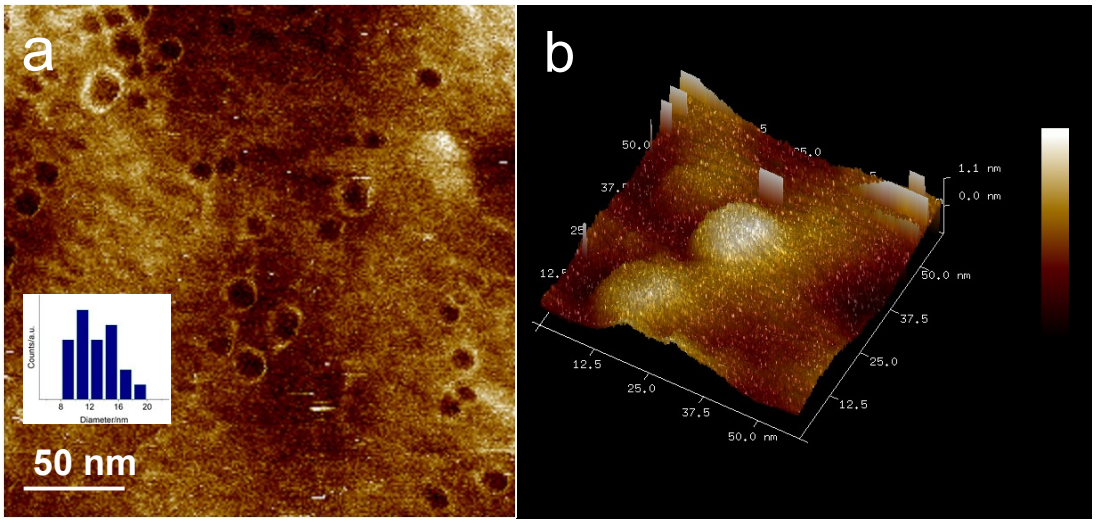

Figure S2. AFM images of FeN/GQDs. a) Phase plot shows the diameter distribution of FeN/GQDs, b) 3D height plot shows a ~0.8 nm height and the number of graphene layers of FeN/GQDs.

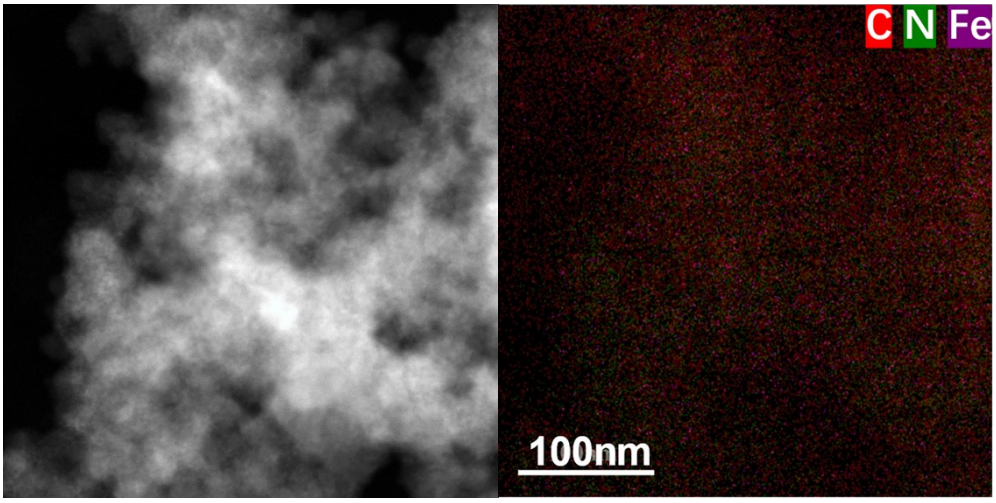

Figure S3. Additional EDS mapping of FeN/GQDs.: the morphology and full element mapping (Red as Carbon, Green as Nitrogen, Purple as Iron).

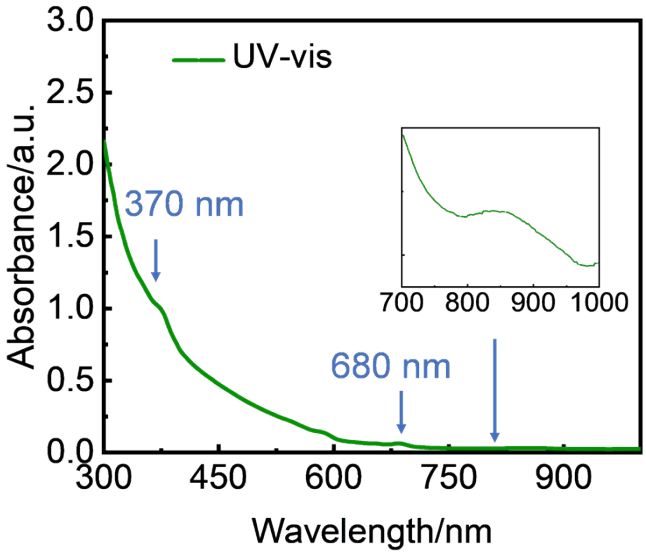

Figure S4. UV-vis spectra of FeN/GQDs. The peak at 370 nm corresponds to the Π-Π* transition of the sp2 domain of graphene. Additionally, two distinct absorption peaks are observed in the near-infrared (NIR) region, with wavelengths of 680 nm in the NIR-I window and 850 nm in the NIR-II window.

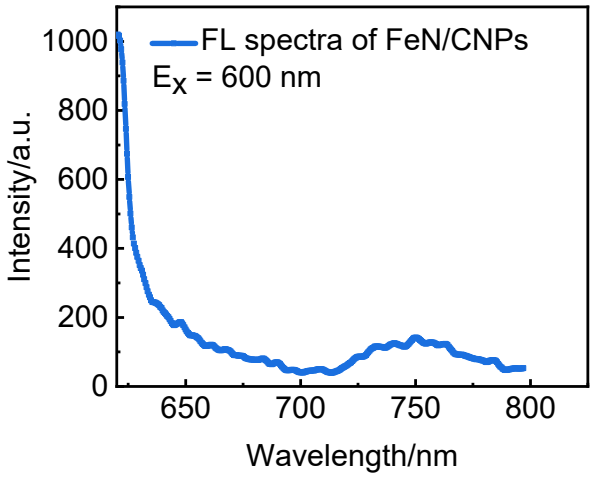

Figure S5. Fluorescence spectra of FeN/GQDs. FeN/GQDs has the only maximum emission peak located at 750 nm when excited at 600 nm, with a stokes shift is of 150 nm.

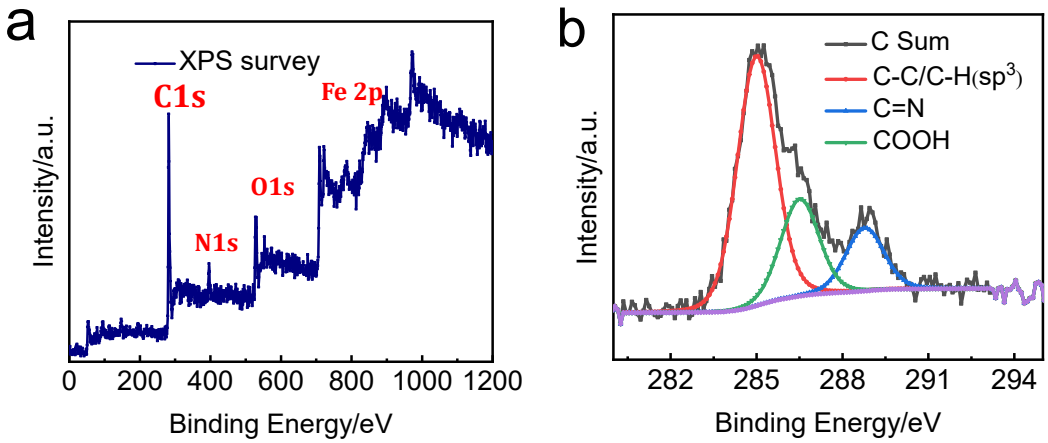

Figure S6. Additional XPS data of FeN/GQDs. a). XPS full survey spectrum of FeN/GQDs; b). XPS C1s spectrum of FeN/GQDs. Three main peaks at 285 eV, 287 eV, and 289 eV, which were assigned to sp^2 C, O-C=O, and C=N, respectively.

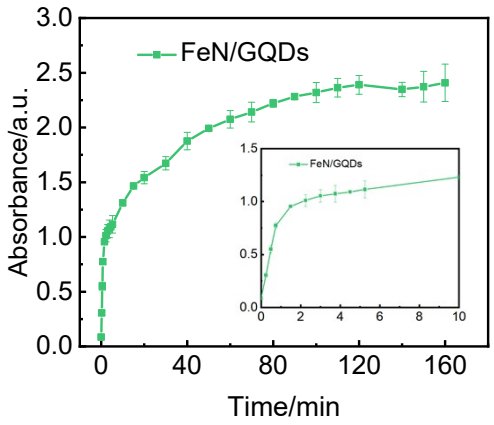

Figure S7. The absorbance at 652nm as a function of time upon addition of H_2O_2 to the FeN/GQDs/TMB solution. The concentration of each component in the solution: FeN/GQDs: 10μg/mL; TMB: 0.3mM; H_2O_2: 10 μM; NaAc-Hac buffer: 1 mL of 0.1M, pH 3.7. Inset: from 0-10

mins

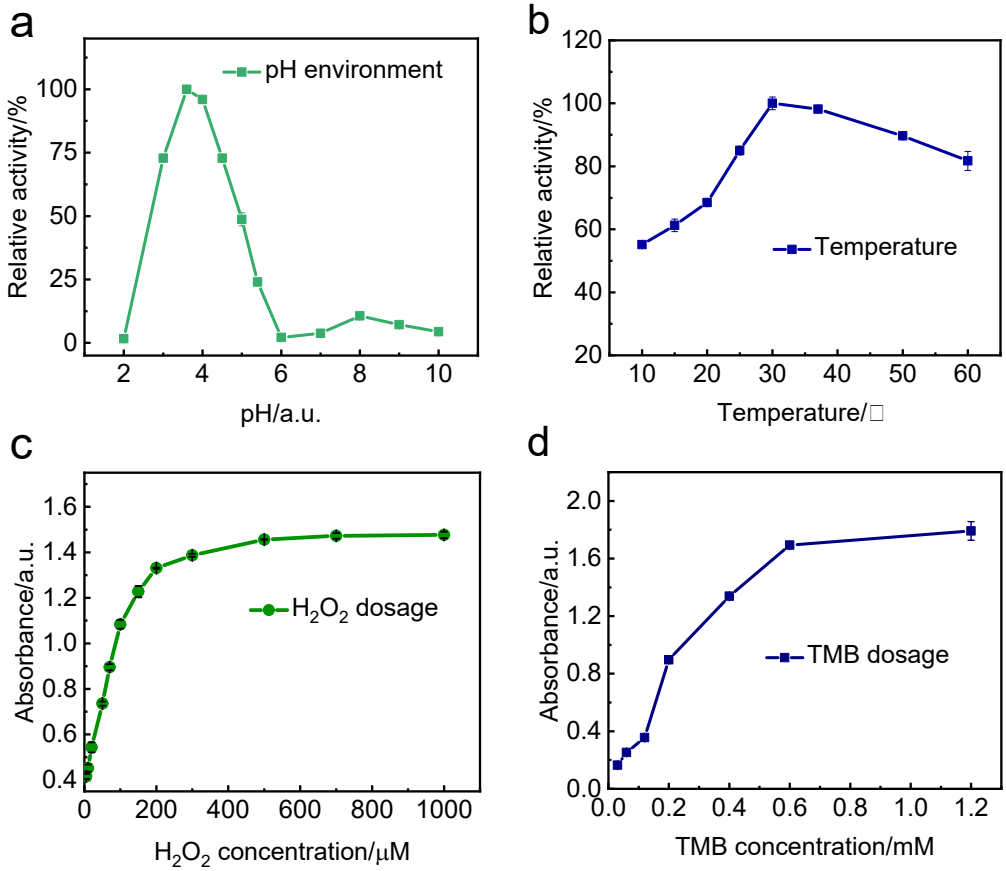

Figure S8. The influence of reaction conditions on the peroxidase-like activity of FeN/GQDs. Relative POD-like reaction activity of FeN/GQDs as a function of (a) pH (2–10 and (b) Temperature (17–60℃). The UV-vis absorbance of FeN/GQDs at 652 nm as a function of (c) H_2O_2 dosage and (d) TMB dosage.

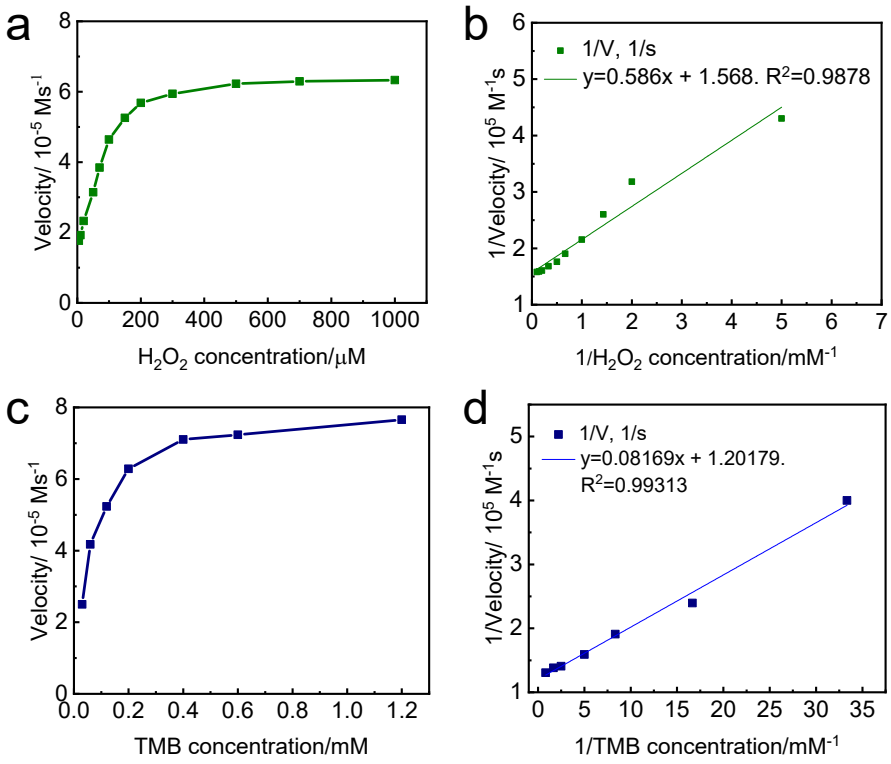

Figure S9. The steady state kinetic analysis for FeN/GQDs under various conditions. Y axis as molar concentration to a certain time (6 mins), represents the change in substrate concentration (H_2O_2/TMB) per unit time, that is, the reaction rate. X-axis indicates the molar concentration of substrates. In here, the plots will reveal the relationship between the substrate concentration (being catalyzed) to the reaction rate, and further get the kinetic constant of the nanozymes (a) [TMB] = 0.4 mM; [H_2O_2]=5-100μM, (c) [H_2O_2]=10μM; [TMB] = 0.05-1.2 mM; (b) and (d) are the Lineweaver-Burk double reciprocal plots corresponding to conditions (a) and (c). The reaction was carried out with 10 μg/mL catalyst of 0.1 M Hac-NaAc buffer, pH=3.6, and temperature=37 °C.

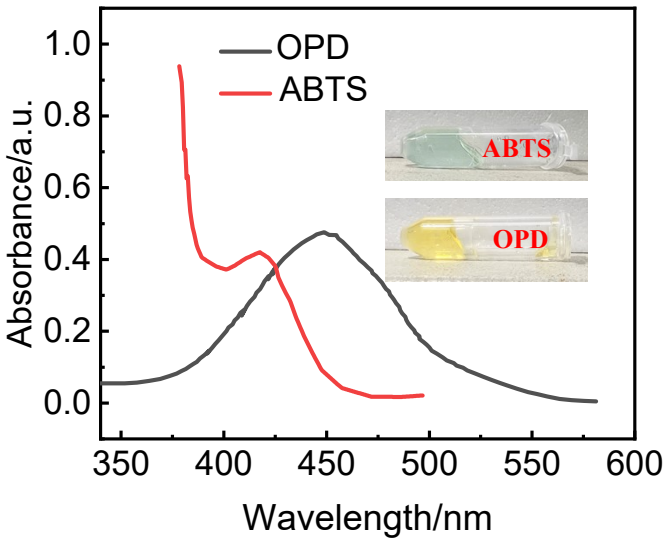

Figure S10. POD-like activity of FeN/GQDs assessed using UV-vis spectroscopy based on different substrates (OPD, ABTS). The UV-vis absorbance of FeN/GQDs solution with OPD and ABTS as

substrates. The concentration of each component in the solution: FeN/GQDs: 10 μg/mL; OPD/ABTS: 0.3mM; H_2O_2: 10μM; NaAc-Hac buffer: 1 mL of0.1M, pH 3.7. Inset: images for color change with ABTS and OPD

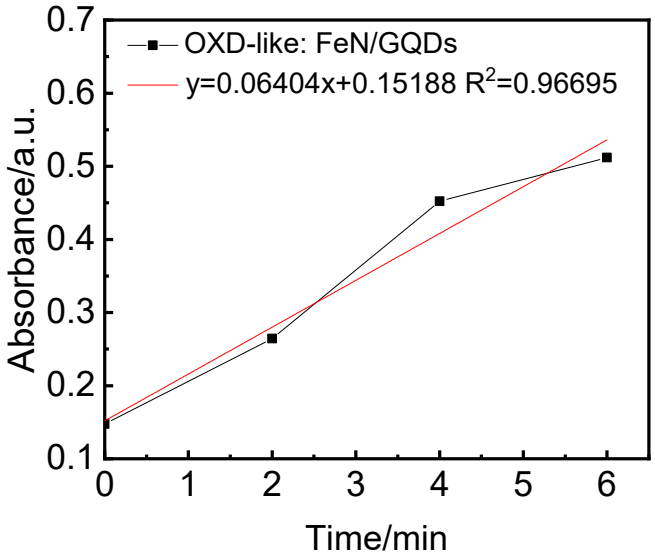

Figure S11. The oxidase – like (OXD-like) activity of FeN/GQDs assessed by measuring the absorbance at 652 nm as a function of time. The concentration of each component in the FeN/GQDs solution: FeN/GQDs: 10μg/mL; TMB: 0.3 mM; NaAc-Hac buffer: 1 mL of 0.1M, pH 3.7.

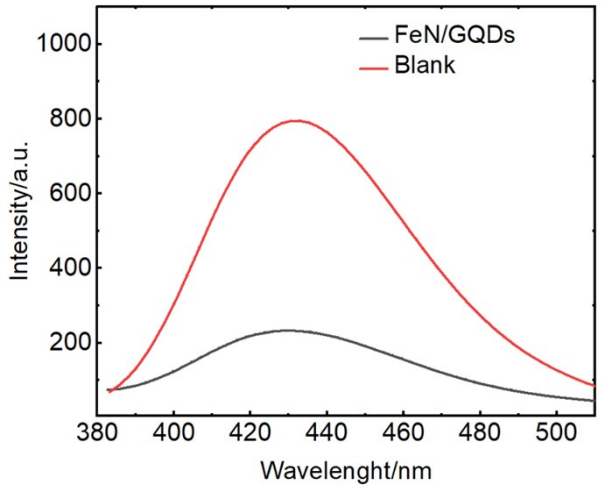

Figure S12. The catalase-like (CAT-like) activity of FeN/GQDs assessed by measuring the fluorescence at 425nm. The concentration of each component: FeN/GQDs: 10ug/mL, TA:0.625mM, H2O2: 10mM, PBS buffer: 0.1M of 1mL, pH7.4.

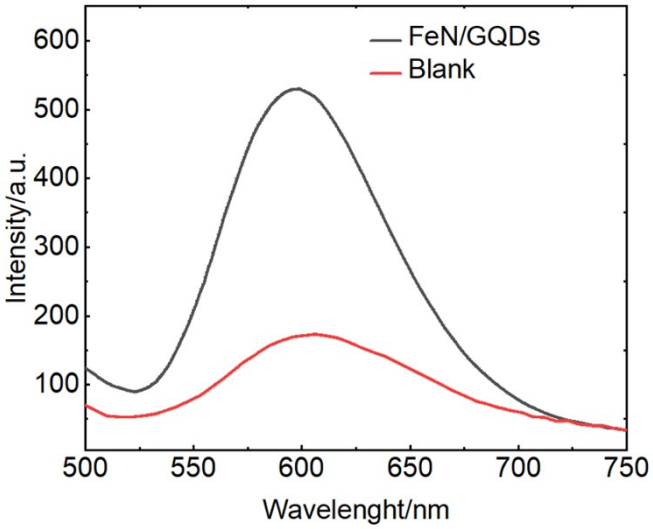

Figure S13. The Superoxide dismutase-like (SOD-like) activity of FeN/GQDs assessed by measuring the fluorescence at 625nm. The concentration of each component: xanthine: 0.6mM, xanthine oxidase: 0.5 U/mL, HE: 0.2 mg/mL, FeN/GQDs: 10μg, PBS buffer: 1mL of 0.1M, pH7.4.

Table S1. EXAFS data fitting results of FeN/GQDs. (S0 2 = 0.75)

Sample	Path	CN	R(Å)	σ 2 (10 -3 Å 2)	ΔE 0 (eV)	R-factor
FeN/GQDs	Fe-N	4.6	2.04	6.6	2.3	0.01

Table S2. Comparison of the kinetic parameters (V_{max} and K_m values) of FeN/GQDs with other nanozymes.

Materials	Substrate	K_m(mM)	V_{max}($M^{-1}S^{-1}$)
FeN/GQDs	TMB	0.52	$6.37*10^{-6}$
	H_2O_2	0.49	$8.32*10^{-6}$
Fe_3O_4[2]	TMB	31.2	$1.614*10^{-6}$
	H_2O_2	2.995	$0.9193*10^{-6}$
FeSSN[3]	TMB	0.53	$2.04*10^{-7}$
	H_2O_2	0.36	$1.32*10^{-7}$
Fe-N-C[4]	TMB	3.6	$3.56*10^{-7}$
	H_2O_2	12.2	$8.60*10^{-8}$
Fe3O4@Cu/GMP–Gox[5]	TMB	15.37	$9.06*10^{-8}$

	H_2O_2	6.35	$3.85*10^{-8}$
g-C_3N_4/PdNPs/ Fe_3O_4NPs[6]	TMB	1.05	$9.58*10^{-6}$
	H_2O_2	7.71	1.26*10-[5]
Fe-Sazyme[7]	TMB	0.3	$18.35*10^{-8}$
	H_2O_2	0.21	$9.94*10^{-8}$
Fe_3O_4[8]	TMB	530	$3.44*10^{-8}$
	H_2O_2	8.8	$9.78*10^{-8}$
HRP[8]	TMB	0.434	$1.00*10^{-7}$
	H_2O_2	3.7	$8.71*10^{-8}$

Table S3. Comparison of glucose detection performance of different nanozymes: detection range, detection limits, and detection time.

Nanozymes	Detection Method	Functionalized molecules	Substrate	Detection Range	Detection Limits	Assay Time
Au NPs/Ag NPs[9]	CM[a]	/	0	5–70 μM	3 μM	40 min
Au@BSA NPs[10]	CM	/	TMB	1–300 μM	0.6 μm	30 min
Au@PNIPAm[11]	CM	/	TMB	10-70 mM	5.07 mM	20 min
Cu-Pt bimetallic fabrics[12]	CM	/	TMB	1–12.5 mM	0.84 mM	5 min
GO/AuNPs[13]	CM	/	TMB	2-30 μM	0.473 μM	60 min
PtNZs[14]	CM	/	TMB	10–1000μM	3.9 μM	15 min
Fe-MOF-Gox[15]	CM	/	TMB	1–500 μM	0.487 μM	30 min
Fe_3O_4 NPs[16]	CM	/	TMB	0.05–4 mM		10 min
Au (BiSA@Au)[17]	CM	/	TMB	80 -1000 μM	43.2 μM	30 min
g-C_3N_4@CuMOFs[18]	FM[b]	/	TA	0.1-22 μM	0.059 μM	30 min

Ag@AuNPs–GO[19]	SERS[c]	4-MPBA	/	2–6 mM	0.33 mM	15 min
Bimetallic film over nanospheres[20]	SERS	4-MPBA/Os-BA	/	0.1–10 mM	0.1 mM	60 min
AgNP/PATP–PMBA[21]	SERS	PMBA/Os-BA	/	0.5–10 mM	0.03 mM	180 min
GOD/AuNPs/GO/GFME[22]	CV[d]	/	/	10-15 μM	1.2 μM	/
Gox-PABA-gFETs[23]	CV	/	/	10-1000 μM	4.1 μM	/
rGO/Cu–Cu_2O[24]	CV	/	/	0.01-7 μM	0.06 μM	/
FeN/GQDs*	CM		TMB	1-100μM	0.78uM	6 min

a: Colorimetric

b: Fluorometric

c: Surface-enhanced Raman Spectra

d: Cyclic Voltammetry

***:** This work.

References

1. Stephen, Z. R.; Dayringer, C. J.; Lim, J. J.; Revia, R. A.; Halbert, M. V.; Jeon, M.; Bakthavatsalam, A.; Ellenbogen, R. G.; Zhang, M. J. A. a. m.; interfaces, Approach to rapid synthesis and functionalization of iron oxide nanoparticles for high gene transfection. **2016,** *8* (10), 6320-6328.
2. Dong, H.; Du, W.; Dong, J.; Che, R.; Kong, F.; Cheng, W.; Ma, M.; Gu, N.; Zhang, Y. J. N. C., Depletable peroxidase-like activity of Fe3O4 nanozymes accompanied with separate migration of electrons and iron ions. **2022,** *13* (1), 5365.
3. Chen, M.; Zhou, H.; Liu, X.; Yuan, T.; Wang, W.; Zhao, C.; Zhao, Y.; Zhou, F.; Wang, X.; Xue, Z. J. S., Single iron site nanozyme for ultrasensitive glucose detection. **2020,** *16* (31), 2002343.
4. Jiao, L.; Xu, W.; Yan, H.; Wu, Y.; Liu, C.; Du, D.; Lin, Y.; Zhu, C. J. A. C., Fe–N–C single-atom nanozymes for the intracellular hydrogen peroxide detection. **2019,** *91* (18), 11994-11999.
5. Wang, X.; Xiong, T.; Cui, M.; Guan, X.; Yuan, J.; Wang, Z.; Li, R.; Zhang, H.; Duan, S.; Wei, F. J. A. M. T., Targeted self-activating Au-Fe3O4 composite nanocatalyst for enhanced precise hepatocellular carcinoma therapy via dual nanozyme-catalyzed cascade reactions. **2020,** *21*, 100827.
6. Zhang, X.; Sun, C.; Li, R.; Jin, X.; Wu, Y.; Fu, F. J. A. C., Dual-Loading of Fe3O4 and Pd Nanoparticles on g-C3N4 Nanosheets Toward a Magnetic Nanoplatform with Enhanced Peroxidase-like Activity for Loading Various Enzymes for Visual Detection of Small Molecules. **2023**.
7. Zhou, X.; Wang, M.; Chen, J.; Xie, X.; Su, X. J. A. C. A., Peroxidase-like activity of Fe–N–C single-atom nanozyme based colorimetric detection of galactose. **2020,** *1128*, 72-79.

8. Gao, L.; Zhuang, J.; Nie, L.; Zhang, J.; Zhang, Y.; Gu, N.; Wang, T.; Feng, J.; Yang, D.; Perrett, S. J. N. n., Intrinsic peroxidase-like activity of ferromagnetic nanoparticles. **2007,** *2* (9), 577-583.
9. Gao, Y.; Wu, Y.; Di, J. J. S. A. P. A. M.; Spectroscopy, B., Colorimetric detection of glucose based on gold nanoparticles coupled with silver nanoparticles. **2017,** *173*, 207-212.
10. Zhang, H.; Liang, X.; Han, L.; Li, F. J. S., "Non-Naked" gold with glucose oxidase-like activity: a nanozyme for tandem catalysis. **2018,** *14* (44), 1803256.
11. Muhammad, P.; Hanif, S.; Li, J.; Guller, A.; Rehman, F. U.; Ismail, M.; Zhang, D.; Yan, X.; Fan, K.; Shi, B. J. N. T., Carbon dots supported single Fe atom nanozyme for drug-resistant glioblastoma therapy by activating autophagy-lysosome pathway. **2022,** *45*, 101530.
12. Prasad, S. N.; Anderson, S. R.; Joglekar, M. V.; Hardikar, A. A.; Bansal, V.; Ramanathan, R. J. B.; Bioelectronics, Bimetallic nanozyme mediated urine glucose monitoring through discriminant analysis of colorimetric signal. **2022,** *212*, 114386.
13. Song, D.; Yang, Y.; Zhou, T.; Liu, Y.; Song, S.; Zhang, J.; Lu, H.; Zhao, Z. J. C., Hybrid hydrogels based on insitu interpenetrating networks graphene oxide (GO) and Au nanoparticles, and its application as peroxidase mimetics for glucose detection. **2018,** *3* (36), 10259-10264.
14. Park, J. S.; Choi, J. S. J. S.; Chemical, A. B., Platinum nanozyme-hydrogel composite (PtNZHG)-impregnated cascade sensing system for one-step glucose detection in serum, urine, and saliva. **2022,** *359*, 131585.
15. Xu, W.; Jiao, L.; Yan, H.; Wu, Y.; Chen, L.; Gu, W.; Du, D.; Lin, Y.; Zhu, C. J. A. a. m.; interfaces, Glucose oxidase-integrated metal–organic framework hybrids as biomimetic cascade nanozymes for ultrasensitive glucose biosensing. **2019,** *11* (25), 22096-22101.
16. Vallabani, N. S.; Karakoti, A. S.; Singh, S. J. C.; Biointerfaces, S. B., ATP-mediated intrinsic peroxidase-like activity of Fe3O4-based nanozyme: one step detection of blood glucose at physiological pH. **2017,** *153*, 52-60.
17. Yan, H.; Jiao, L.; Wang, H.; Zhu, Y.; Chen, Y.; Shuai, L.; Gu, M.; Qiu, M.; Gu, W.; Zhu, C. J. S.; Chemical, A. B., Single-atom Bi-anchored Au hydrogels with specifically boosted peroxidase-like activity for cascade catalysis and sensing. **2021,** *343*, 130108.
18. Bagheri, N.; Dastborhan, M.; Khataee, A.; Hassanzadeh, J.; Kobya, M. J. S. A. P. A. M.; Spectroscopy, B., Synthesis of g-C3N4@ CuMOFs nanocomposite with superior peroxidase mimetic activity for the fluorometric measurement of glucose. **2019,** *213*, 28-36.
19. Gupta, V. K.; Atar, N.; Yola, M. L.; Eryılmaz, M.; Torul, H.; Tamer, U.; Boyacı, İ. H.; Üstündağ, Z. J. J. o. c.; science, i., A novel glucose biosensor platform based on Ag@ AuNPs modified graphene oxide nanocomposite and SERS application. **2013,** *406*, 231-237.
20. Kong, K. V.; Lam, Z.; Lau, W. K. O.; Leong, W. K.; Olivo, M. J. J. o. t. A. C. S., A transition metal carbonyl probe for use in a highly specific and sensitive SERS-based assay for glucose. **2013,** *135* (48), 18028-18031.
21. Bi, X.; Du, X.; Jiang, J.; Huang, X. J. A. c., Facile and sensitive glucose sandwich assay using in situ-generated Raman reporters. **2015,** *87* (3), 2016-2021.
22. Han, Z.; Zhang, X.; Yuan, H.; Li, Z.; Li, G.; Zhang, H.; Tan, Y. J. J. o. P. S., Graphene oxide/gold nanoparticle/graphite fiber microelectrodes for directing electron transfer of glucose oxidase and glucose detection. **2022,** *521*, 230956.
23. Fenoy, G. E.; Marmisollé, W. A.; Knoll, W.; Azzaroni, O. J. S.; Diagnostics, Highly sensitive urine glucose detection with graphene field-effect transistors functionalized with

electropolymerized nanofilms. **2022,** *1* (1), 139-148.

24. Preechakasedkit, P.; Nawaukkaratharnant, N.; Teekayupak, K.; Lomae, A.; Ruecha, N. J. J. o. S. A. M.; Devices, Single-preparation rGO/Cu–Cu2O nanocomposite-modified electrode integrating NaOH immobilized polymer blend film for one-step nonenzymatic glucose detection. **2023,** *8* (2), 100535.